Supporting Information for Koehl et al. (2023 – TEKTONIKA)

Timanian Fold-and-thrust Belt and Caledonian Overprint in the Selis Ridge Imaged by New 3D Seismic Attributes and Spectral Decomposition

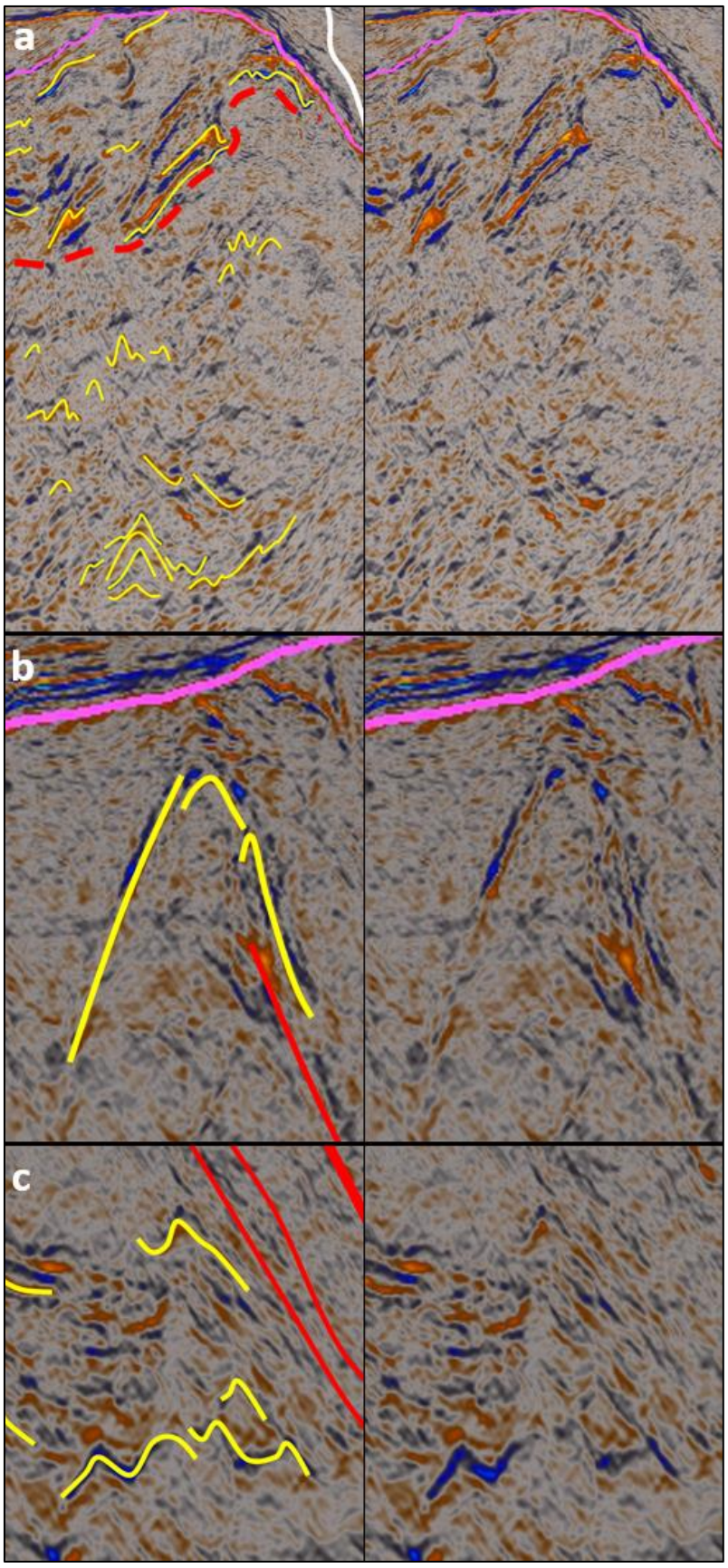

Figure SI-1: (a) Interpreted (left hand-side inset) and uninterpreted (right hand-side inset) showing symmetrical upright folds within meta-igneous rocks of the central segment of the Selis Ridge in the footwall of the main shear zone. See location in Figure 7 and legend in Figure 2. (b) and (c) Interpreted (left hand-side inset) and uninterpreted (right hand-side inset) showing a symmetrical upright folds in meta-igneous rocks of the central (b) and southernmost (c) segments of the Selis Ridge. See locations in Figure 5 and legend in Figure 2.

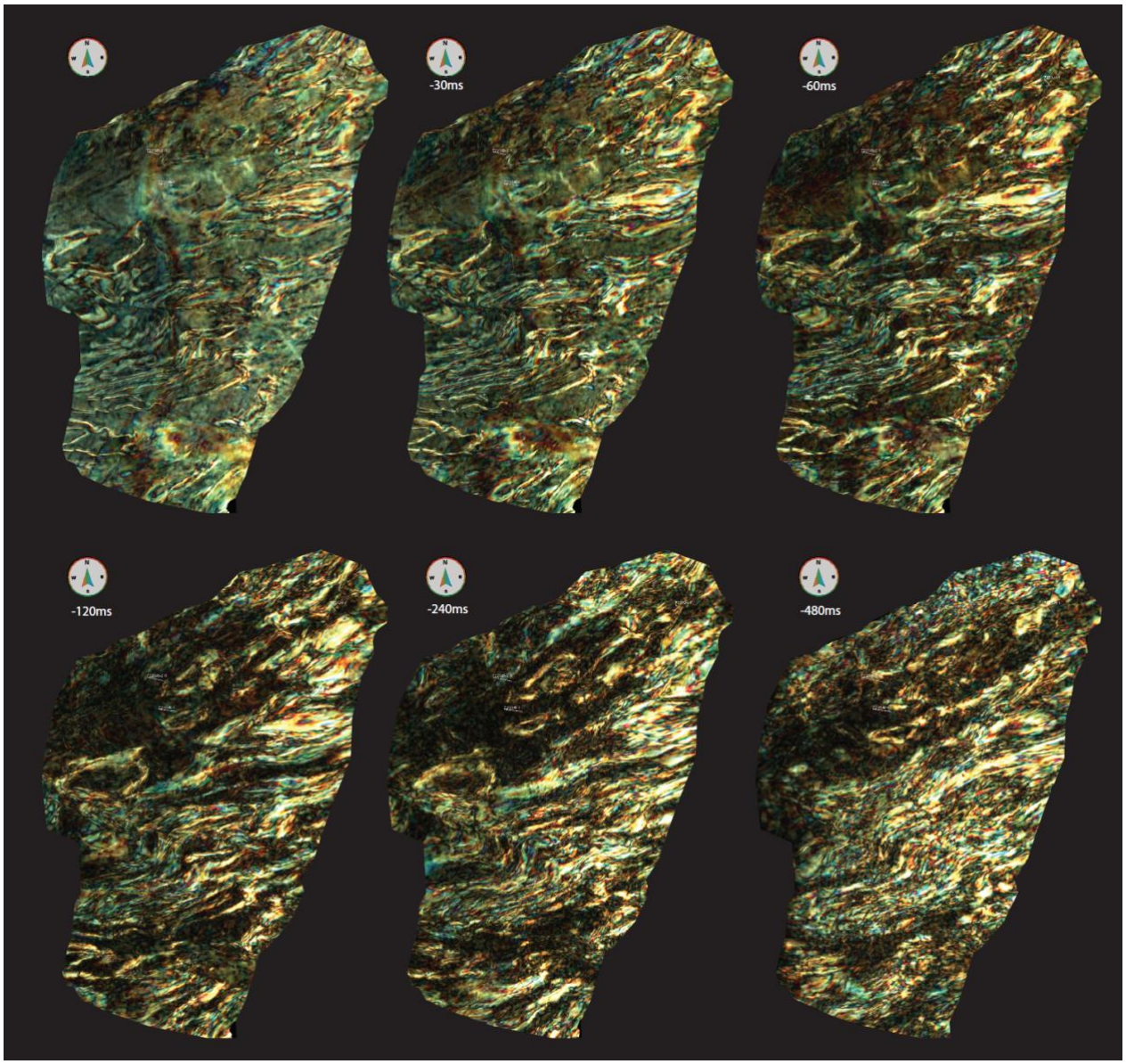

Figure SI-2: Time-slices through the 3D seismic dataset showing the vertical continuity of oval-shaped fold structures. The upper left surface corresponds to the main post-Caledonian unconformity (i.e., Top-basement reflection).

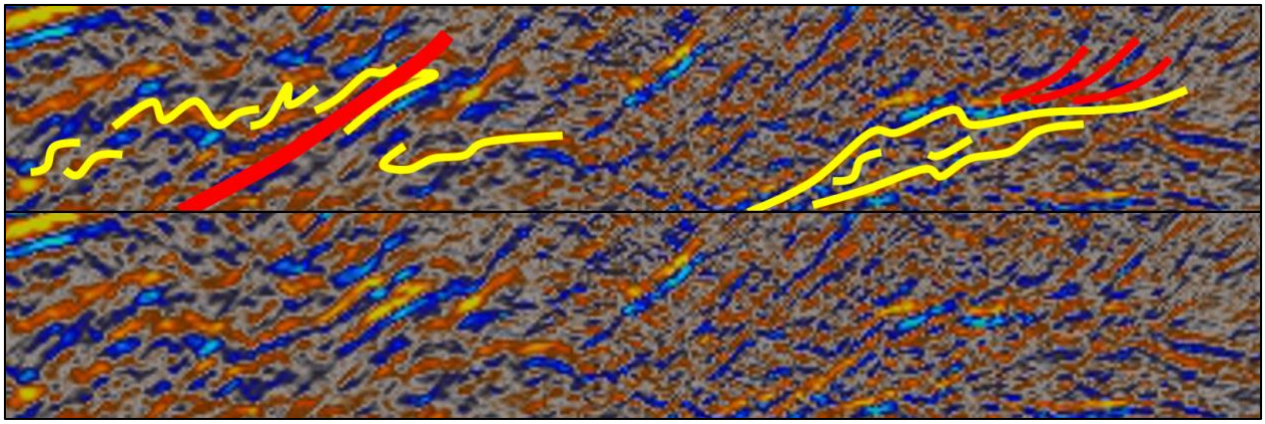

Figure SI-3: Interpreted (upper inset) and uninterpreted (lower inset) zoom in seismic data showing potential antiformal thrust stack and imbricate thrusts in the north (right hand-side) and potential duplex and thrust with top-north reverse offset in the south (left hand-side). Location is displayed in Figure 2.

Section SI-1: Exploration wells 7220/6-1 and 7220/6-2R

Exploration wells 7220/6-1 and 7220/6-2R both penetrated basement rocks in the Selis Ridge. The former ended in quartzite and the latter penetrated quartz- and plagioclase-dominated and K-feldspar-poor, dark green rocks with varying degrees of deformation and metamorphic grade (Figure 1 supplement 4). Notably, the dark green rocks in well 7220/6-2R show bands of (1) highly foliated, coarse-grained, poorly-sorted, chlorite-rich and (2) fine-grained, moderately-sorted, biotite-rich material, and (3) bands of foliated rocks crosscut by cracks filled with angular clasts of quartz- and plagioclase-rich rocks partly cemented with calcite (Figure 1 supplement 4). Well 7220/6-2R penetrated steeply south-dipping, moderate-amplitude reflections in the northern part of the Selis Ridge (Figure 2 supplement 4). The bands of intensely foliated, chlorite-dominated and biotite-dominated may therefore correspond respectively to greenschist-facies, (proto-) mylonitic and greenschist–amphibolite-facies, (ultra-) mylonitic ductile shear zones (possibly phyllonite). By contrast, bands of foliated basement rocks truncated by cracks filled with calcite-cemented clasts likely represent brittle fault zones. Note that the cracks are arcuate, thus possibly suggesting reworking by subsequent ductile deformation events. These observations attest of the strongly deformed character of basement rocks in the Selis Ridge and suggest that the high-amplitude character of seismic reflections in the northern part of the ridge is, at least partly, due to the occurrence of mylonitic bands and shear zones (e.g., Christensen, 1965, 1966; Fountain et al., 1984; Hurich et al., 1985).

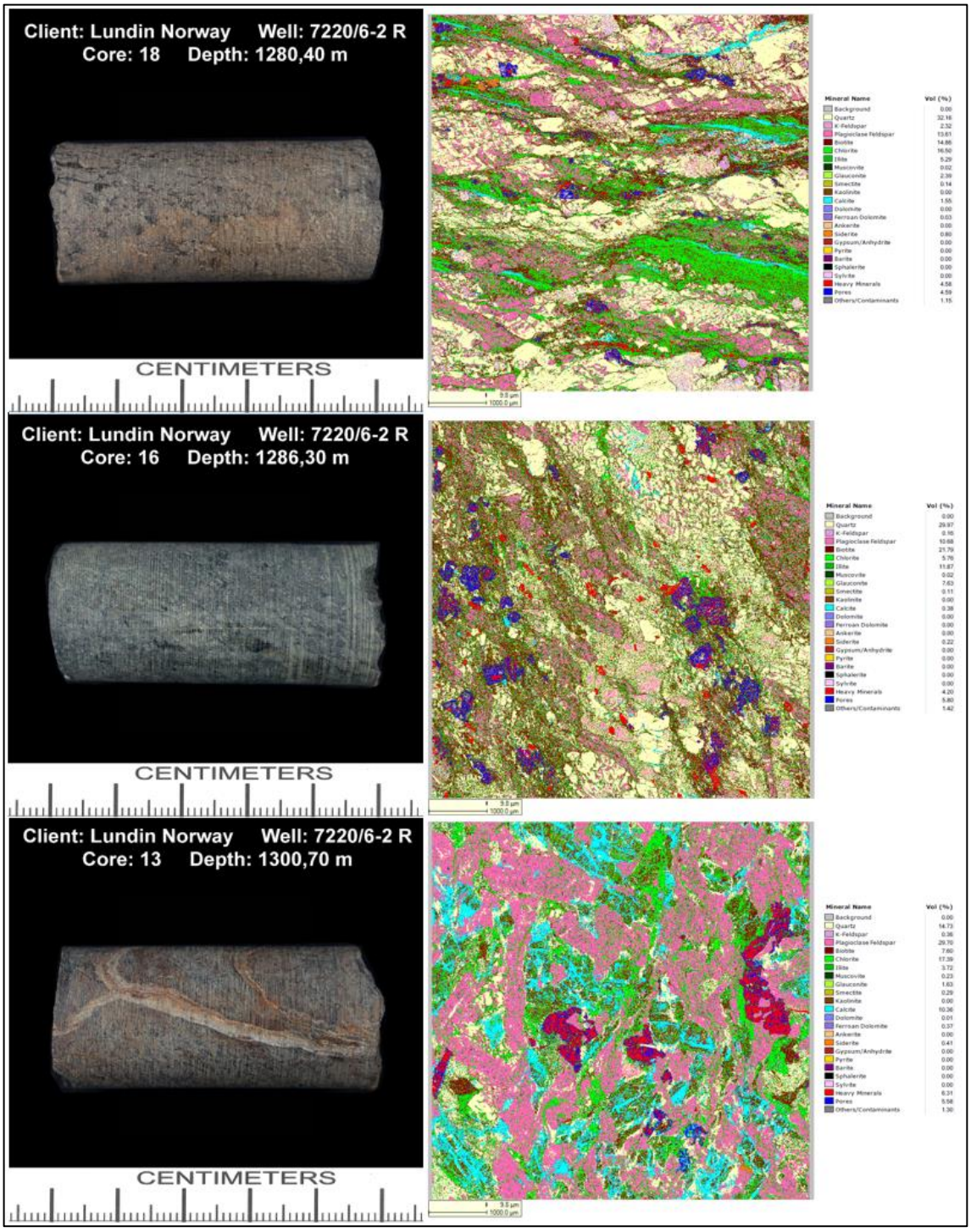

Figure SI-4A: Sidewall cores from well 7220/6-2R (left hand-side column) and Scanning Electron Microscope view of the composition of thin sections of the sidewall cores (right hand-side column).

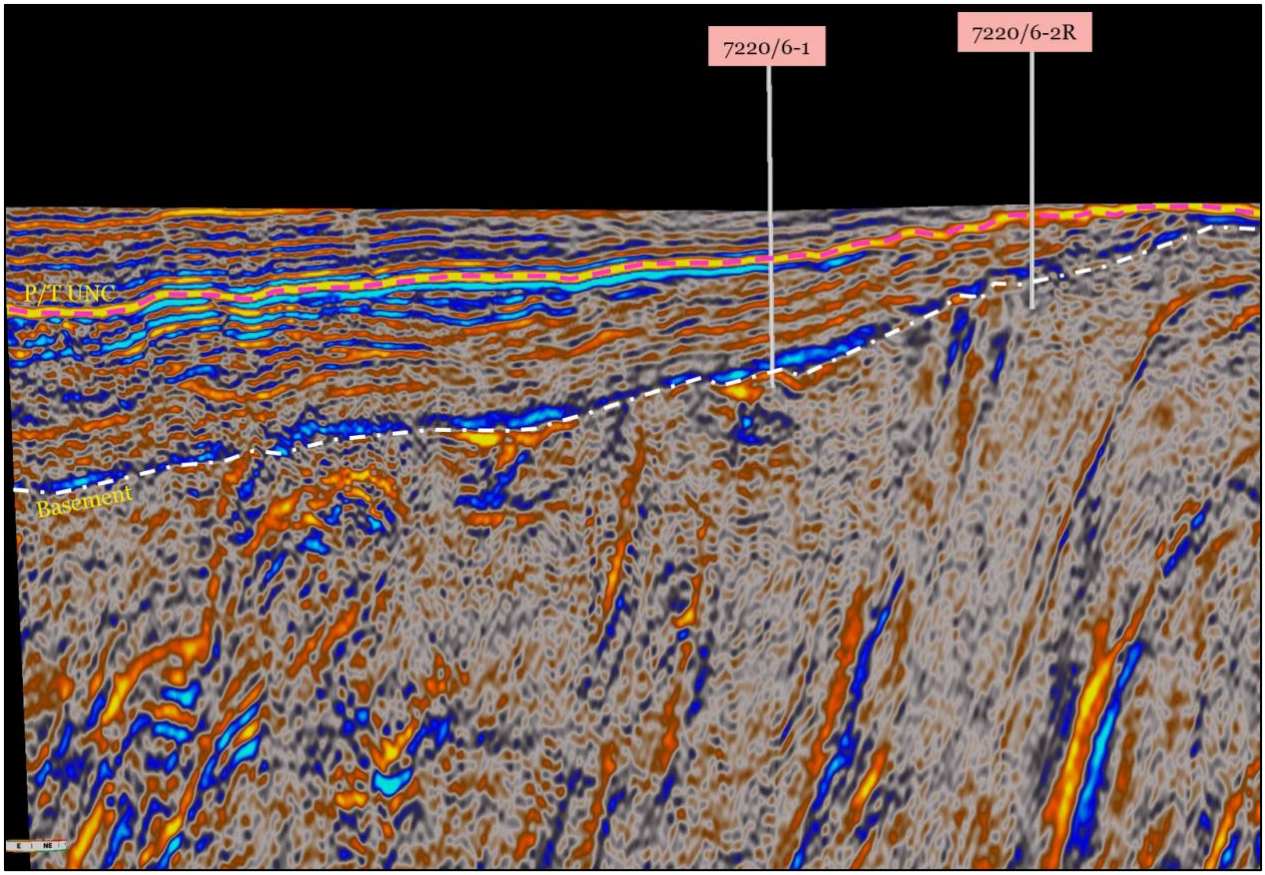

Figure SI-4B: Seismic section through wells 7220/6-1 and 7220/6-2 R showing the relationship between the lithologies penetrated and seismic facies. Quartzite is penetrated by well 7220/6-1 is associated with gently curving sub-horizontal reflections, whereas deformed metasedimentary rocks in well 7220/6-2 R are tied to steeply south-dipping, moderate-amplitude reflections.

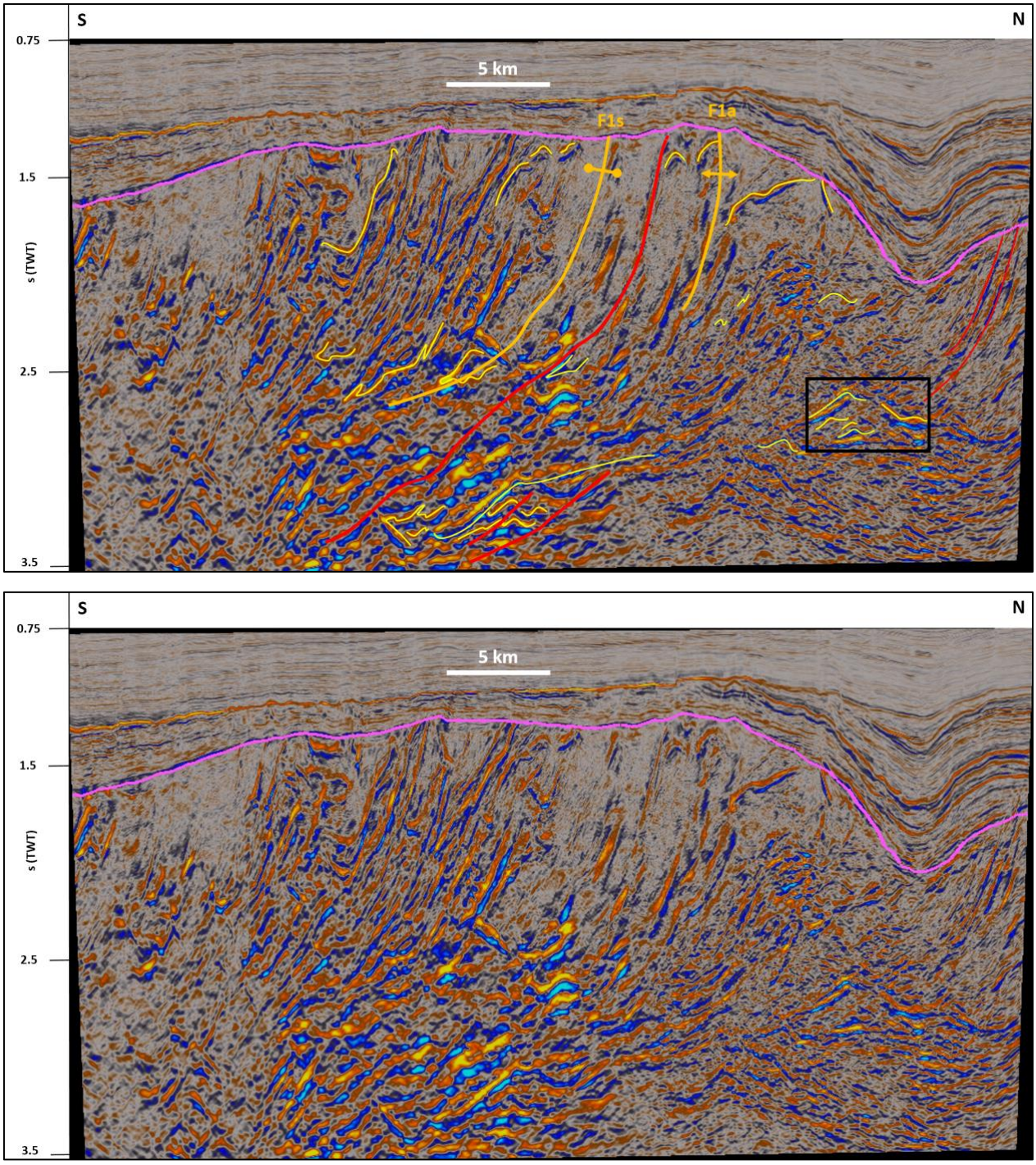

Figure SI-5: Interpreted (upper inset) and uninterpreted (lower inset) N–S seismic section through the northern segment of the Selis Ridge showing major top-north thrusts and related north-verging synforms (e.g., F1s) and antiforms (e.g., F1a). Notice the antiformal thrust stack in the black frame. Location is shown in Figure 1c and legend in Figure 2.

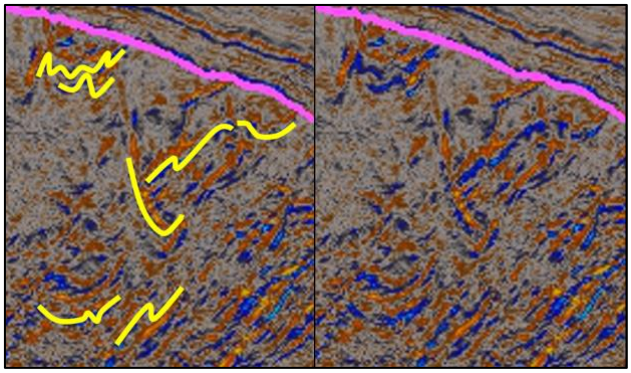

Figure SI-6: Interpreted (left hand-side inset) and uninterpreted (right hand-side inset) zoom in Figure 2 showing upright E–W-trending folds in the northernmost part of the Selis Ridge. Location and legend are shown in Figure 2.

Calculation dip angle main NNE-dipping shear zones

The present depth conversion assumes no significant lateral variations of density in post-Caledonian sedimentary rocks

Density metasedimentary rocks Selis Ridge (from Gernigon et al., 2018) (m.s-1)	6.15

Shear zone between central and northern segments

Figure 2	max	min	
distance shallowest and deepest portion shear zone along dip direction (NNE-SSW) (km)		10	9
differential depth shallowest and deepest portion shear zone along dip direction (NNE-SSW) (s TWT)		2	
differential depth shallowest and deepest portion shear zone along dip direction (NNE-SSW) (km)		6.15	
	min	max	
dip angle shear zone (rad)		0.55	0.60
dip angle shear zone (deg)		31.6	34.3

Figure 5	max	min	
distance shallowest and deepest portion shear zone along dip direction (NNE-SSW) (km)		5	4.5
differential depth shallowest and deepest portion shear zone along dip direction (NNE-SSW) (s TWT)		1.5	
differential depth shallowest and deepest portion shear zone along dip direction (NNE-SSW) (km)		4.6125	
	min	max	
dip angle shear zone (rad)		0.75	0.80
dip angle shear zone (deg)		42.7	45.7

Figure 15		
distance shallowest and deepest portion shear zone along dip direction (NNE-SSW) (km)	10	
differential depth shallowest and deepest portion shear zone along dip direction (NNE-SSW) (s TWT)	2.2	
differential depth shallowest and deepest portion shear zone along dip direction (NNE-SSW) (km)	6.765	
dip angle shear zone (rad)	0.59	
dip angle shear zone (deg)	34.1	

Supplement 1	max	min	
distance shallowest and deepest portion shear zone along dip direction (NNE-SSW) (km)		8	7
differential depth shallowest and deepest portion shear zone along dip direction (NNE-SSW) (s TWT)		2.3	
differential depth shallowest and deepest portion shear zone along dip direction (NNE-SSW) (km)		7.0725	
	min	max	
dip angle shear zone (rad)		0.72	0.79
dip angle shear zone (deg)		41.5	45.3

Compilation all figures and data northern shear zone		
dip angle shear zone (deg)	31.6	45.7

Shear zone between southernmost and southern segments

Figure 4	max	min	
distance shallowest and deepest portion shear zone along dip direction (NNE-SSW) (km)		7	6
differential depth shallowest and deepest portion shear zone along dip direction (NNE-SSW) (s TWT)		2	
differential depth shallowest and deepest portion shear zone along dip direction (NNE-SSW) (km)		6.15	
	min	max	
dip angle shear zone (rad)		0.72	0.80
dip angle shear zone (deg)		41.3	45.7

Details format

Figure number	max	min	
distance shallowest and deepest portion shear zone along dip direction (NNE-SSW) (km)		x(max)	x(min)
differential depth shallowest and deepest portion shear zone along dip direction (NNE-SSW) (s TWT)		y	
differential depth shallowest and deepest portion shear zone along dip direction (NNE-SSW) (km)		z = y/2*6.15	
	min	max	
dip angle shear zone (rad)		α(min) (rad) = tan-1(z/x(max))	α(max) (rad) = tan-1(z/x(min))
dip angle shear zone (deg)		**α(min) (deg)**	**α(max) (deg)**

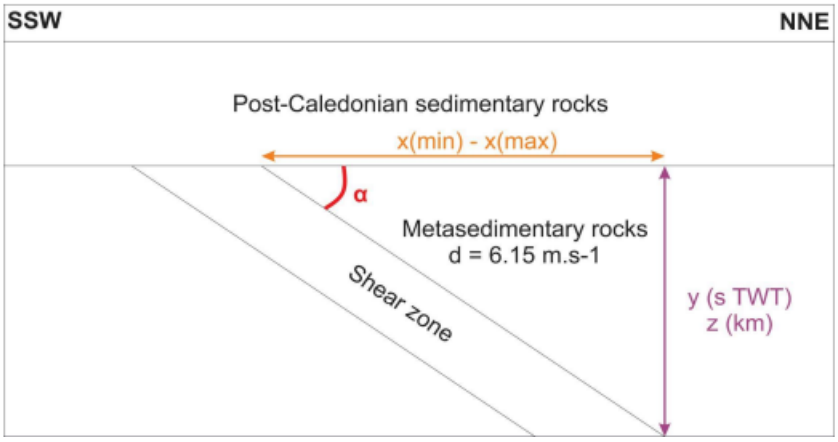

Figure SI-7: Calculation of the dip angle of the main NNE-dipping shear zones in the Selis ridge.

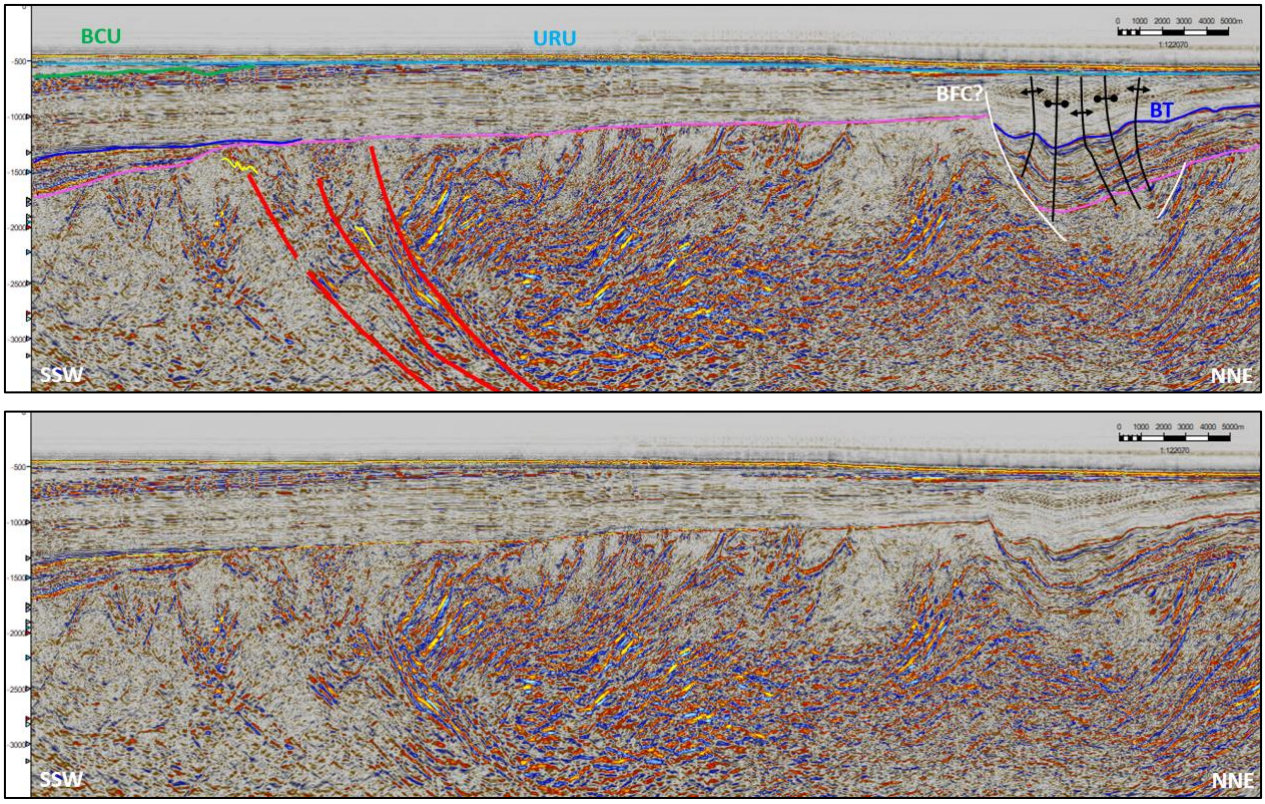

Figure SI-8: Seismic section showing E–W-trending folds in basement rocks and upper Paleozoic–Mesozoic sedimentary successions being truncated by the Upper Regional Unconformity in the hanging wall of the Bjørnøyrenna Fault Complex in the north. Abbreviations: BCU: Base Cretaceous Unconformity; BFC: Bjørnøyrenna Fault Complex; BT: Base Triassic; URU: Upper Regional Unconformity.